Bioorganic & Medicinal Chemistry Letters 27 (2017) 3472–3476

Contents lists available at ScienceDirect

Bioorganic & Medicinal Chemistry Letters

journal homepage: www.elsevier.com/locate/bmcl

Initial evaluation of Cu-64 labeled PARPi-DOTA PET imaging in mice with mesothelioma

Tao Huang [a], Pengcheng Hu [a,b], Anna B. Banizs [a], Jiang He [a,*]

[a] Department of Radiology and Medical Imaging, University of Virginia, Charlottesville, VA 22908, United States
[b] Department of Nuclear Medicine, Zhongshan Hospital, Fudan University, Shanghai 200032, China

ARTICLE INFO

Article history:
Received 19 March 2017
Revised 24 May 2017
Accepted 25 May 2017
Available online 26 May 2017

Keywords:
PARP inhibitor
PET
Imaging
Olaparib
Mesothelioma

ABSTRACT

Poly(ADP-ribose) polymerase (PARP) has emerged as an important molecular target for the treatment of several oncological diseases. A couple of molecular probes based on Olaparib scaffold have been developed by incorporation of F-18 or fluorophore for positron emission tomography (PET) or optical imaging in several types of tumor. PARP has been reported overexpressed in mesothelioma. We hereby synthesized an analogue of Olaparib containing DOTA moiety and radiolabeled it with Cu-64 to evaluate its utility of PET tracer for mesothelioma. The Cu-64 labeling was conveniently achieved at 90% yield with final compound at >99% radiochemistry purity. The biodistribution and PET imaging were performed at 0.5, 1, 2 and 18 h to confirm the in vivo tumor targeting. The tumor uptake in study group was significant higher than that in control group (3.45 ± 0.47% ID/g vs 2.26 ± 0.30% ID/g) and tumor were clearly detected by PET imaging. These results suggest the feasibility to develop an Olaparib-based theranostic agent for mesothelioma.

Poly(ADP-ribose) polymerase is a family of nuclear enzymes that sense DNA damage induced by chemical or ionizing radiation, and participate the repair process by binding to the DNA breaks.[1] In cancer cells with the HR repair pathway deficiency due to BRCA1 and BRCA2 mutation, inhibition of PARP will lead to DNA breaks unrepaired and cause cell death eventually.[2] Therefore, PARP has become a novel target for cancer therapy in the past decades and a variety of small molecule inhibitors of PARP have been developed to treat cancers. These PARP inhibitors are used either as a single agent in cancers with BRCA1 and BRCA2 dysfunction or in combination with DNA damaging therapeutics (radiation or chemotherapy) to improve the therapeutic benefits by blocking the repair.[3] Also, due to the well-established role in the DNA repair and the potential value to be a prognostic indicator, and the fact that the expression levels of PARP enzyme are significantly higher in a variety of tumors compared to normal tissues,[4–8] As such, PARP has become an attractive biomarker for non-invasive PET imaging.

Olaparib (AZD2281), a FDA-approved first class drug for ovarian cancer, is a potent and bioavailable small molecule inhibitor for PARP-1 and PARP-2. Among a library of candidate inhibitors, Olaparib was picked up for further clinical trials based on a comprehensive consideration of potency and pharmacokinetic properties. In terms of potency, a number of candidates hold sub nano-molar IC_{50}.[9] Based on the core scaffold of this molecule, several imaging agents have been developed by incorporation of F-18 or/and BODIPY-FL dye into it (Fig. 1A). ^{18}F-BO was radiolabeled via bio-orthogonal reaction between *trans*-cyclooctenes (TCO) and tetrazine (Tz) and can be used as a companion diagnostic PET tracer to monitor therapeutic effect of PARP1 inhibition.[10–12] PARPi-FL was created by replacing the cyclopropane moiety with the green fluorescent BODIPY-FL. It was mainly used for fluorescent imaging although it could be labeled with F-18 via ion exchange to become a dual-modality agent for both PET and fluorescent imaging. The low specific activity after F-18 labeling and the in vivo defluorination which results in high bone uptake limit its application in PET imaging.[12–14] It should be noted that although both modifications introduced bulky substituents to replace the small cyclopropane moiety, the binding affinities were only slightly affected. Combined with observation from the affinity of the library analogues,[9] it turned out the molecule can tolerate a variety of modification and still keep the potency intact or slightly impacted.

Our lab has been studying malignant mesothelioma (MM) treatment for last decade.[15,16] MM is an asbestos-related tumor that forms in the thin layer of tissue that covers the lung, chest wall, or abdomen. Its prognosis remains poor due to the diagnostic challenge and resistance to conventional therapies. A recent report shows that PARP1 is highly expressed in MM cells, and suggests

* Corresponding author at: 480 Ray C Hunt Dr, PO Box 801339, Department of Radiology and Medical Imaging, University of Virginia, Charlottesville, VA 22903, United States.
E-mail address: jh6qv@virginia.edu (J. He).

http://dx.doi.org/10.1016/j.bmcl.2017.05.077
0960-894X/

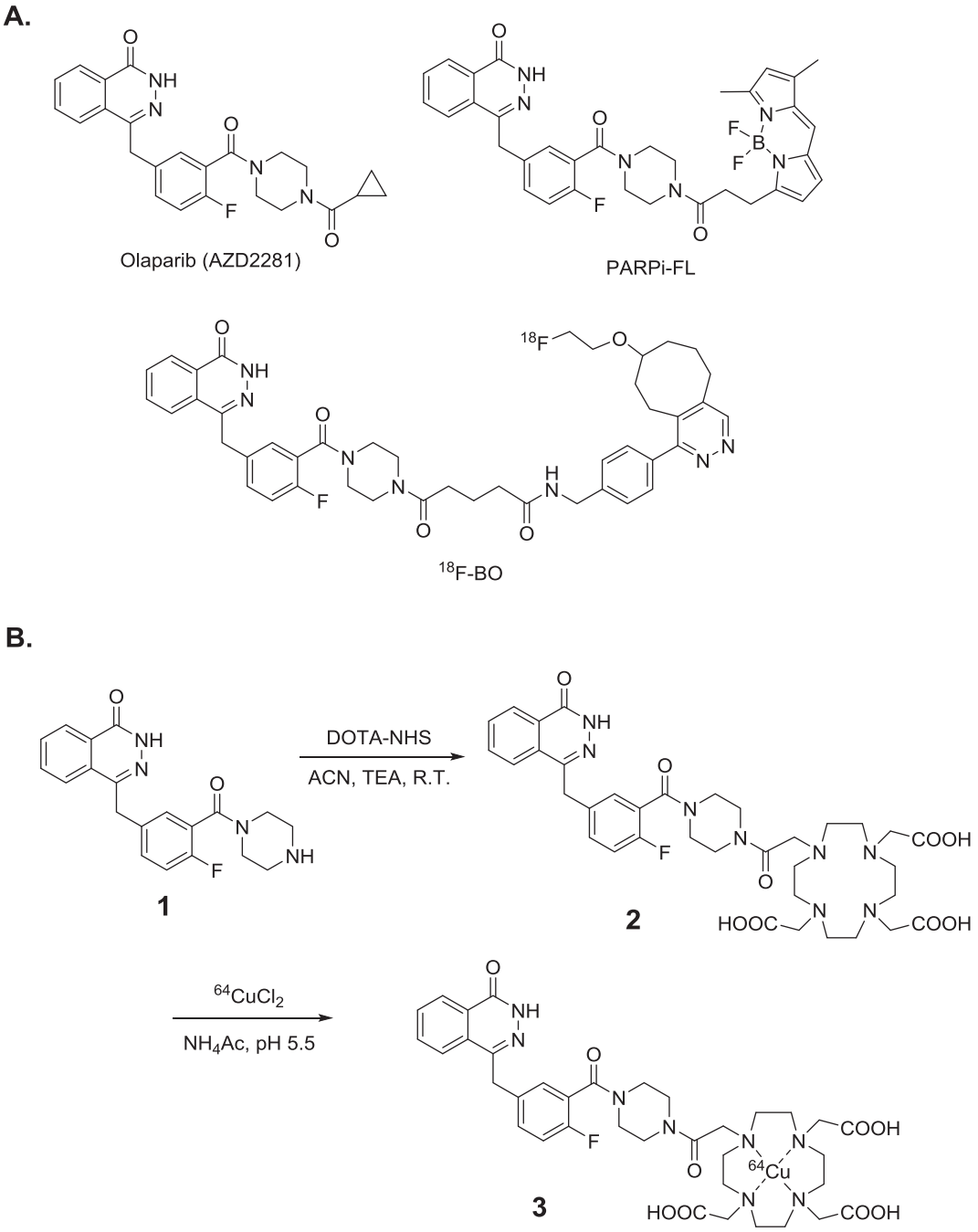

Fig. 1. (A) Structure of Olaparib (AZD2281), PARPi-FL (PET and Fluorescent dual modality probe), and 18F-BO (PET probe); (B) Synthesis of the designed compound **3**.

that chemoresistance to MM treatment may result from a higher level of PARP1-mediated DNA repair.[17] With this regard, we proposed a proof-of-concept study to develop an Olaparib-derived agent targeting PARP for MM imaging or/and therapy. Different from the previous F-18 labeled agents, we would like to modify this molecule with introduction of Cu-64, a PET isotope with favorable characteristics ($T_{1/2}$ = 12.7 h, β^+ 17.4%, E_{max} = 0.656 MeV, β^- 39%, E_{max} = 0.573 MeV).[18] Compared with F-18 ($T_{1/2}$ = 109 min), there is a longer physical half-life for Cu-64 which allow more time for time-sensitive operations. More importantly, Cu-64 or other isotope Cu-67 has therapeutic efficacy[19] by different radiation and therefore, can be used for both PET imaging and radiotherapy. Moreover the radiotherapy effect can be synergistically enhanced by blocking PARP repair pathway.

As outlined in Fig. 1B, the compound **2** was synthesized by incubating a mixture of 4-(4-fluoro-3-(piperazine-1-carbonyl)benzyl) phthalazin-1(2*H*)-one (compound **1**, 73 mg, 0.2 mmol) and 1,4,7,10-tetraazacyclododecane-1,4,7,10-tetraacetic acid mono-*N*-hydroxysuccinimide ester (DOTA-NHS, 153 mg, 0.2 mmol) dissolved in 2 mL acetonitrile (ACN) in the presence of triethylamine (TEA) overnight under room temperature, purified with reverse-phase thin lay tomography (RP-TLC) plate and characterized by MALDI-TOF mass spectroscopy (W.M. Keck Biomedical mass spectrometry laboratory at the University of Virginia). The analyzed *m*/*z* results were $[M+H]^+$ 753.3, $[M+K]^+$ 791.3, which confirmed the successful conjugation. The chemical yield was around 55%.

After conjugation with DOTA, the bioactivity of the compound **2** was assessed following a reported assay,[20] which gave a IC50 of

200 nM. Although the potency is 40-fold less than the parent compound **1**, the compound **2** is still an inhibitor of PARP with decent potency.

The radiolabeling was achieved by adding $^{64}CuCl_2$ (2–3 mCi, 30 μL) to into a solution of the compound **2** (30 μg) in 100 μL ammonium acetate buffer (pH 5.5, 0.1 N) and incubating the mixture at 40 °C for 45 min. The reaction progress was monitored by HPLC analysis. When the radiolabeling was completed, 200 μL ethylenediaminetetraacetic acid (EDTA) solution (0.01 M) was added and the resulting mixture was loaded onto a semi-preparative HPLC (C18 reverse-phase Apollo column, 5 μm, 250 × 10 mm) for purification. The mobile phase changed from 100% Solvent A (0.1% TFA in water) and 0% Solvent B (0.1% TFA, 80% ACN in water) to 100% Solvent B in 30 min at a flow rate of 3 mL/min. The compound **3** was collected with the retention time at 14.0 min with radiochemical yields higher than 90%. And the collected fraction was analyzed with analytical HPLC (C18 reverse-phase Phenomenex Gemini column, 5 μm, 150 × 4.6 mm, mobile phase started

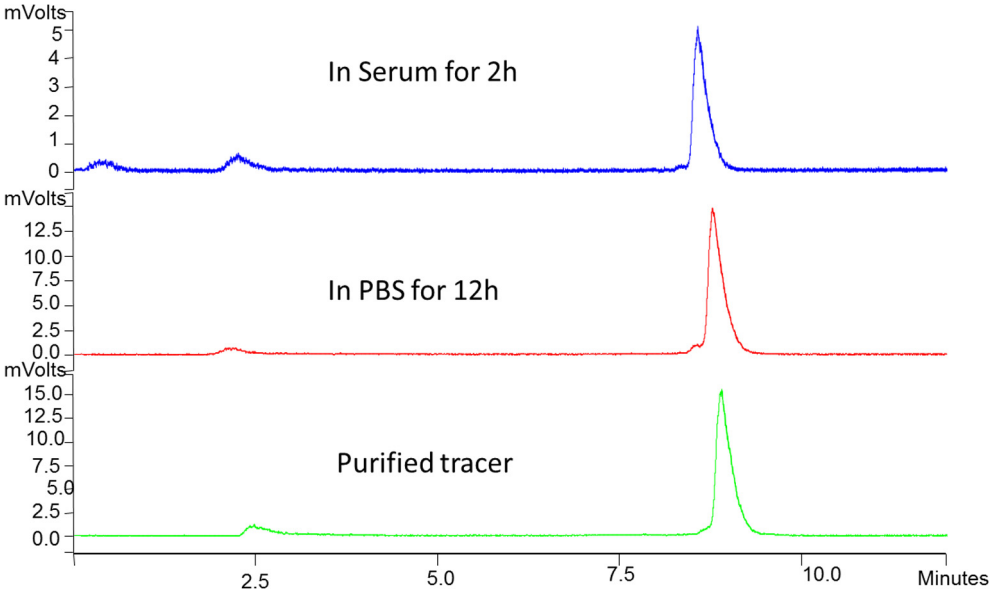

Fig. 2. The HPLC chromatograms of the purified compound **3** (bottom), after incubated in PBS at 37 °C for 12 h (middle), and after incubated in mouse serum at 37 °C for 2 h (top).

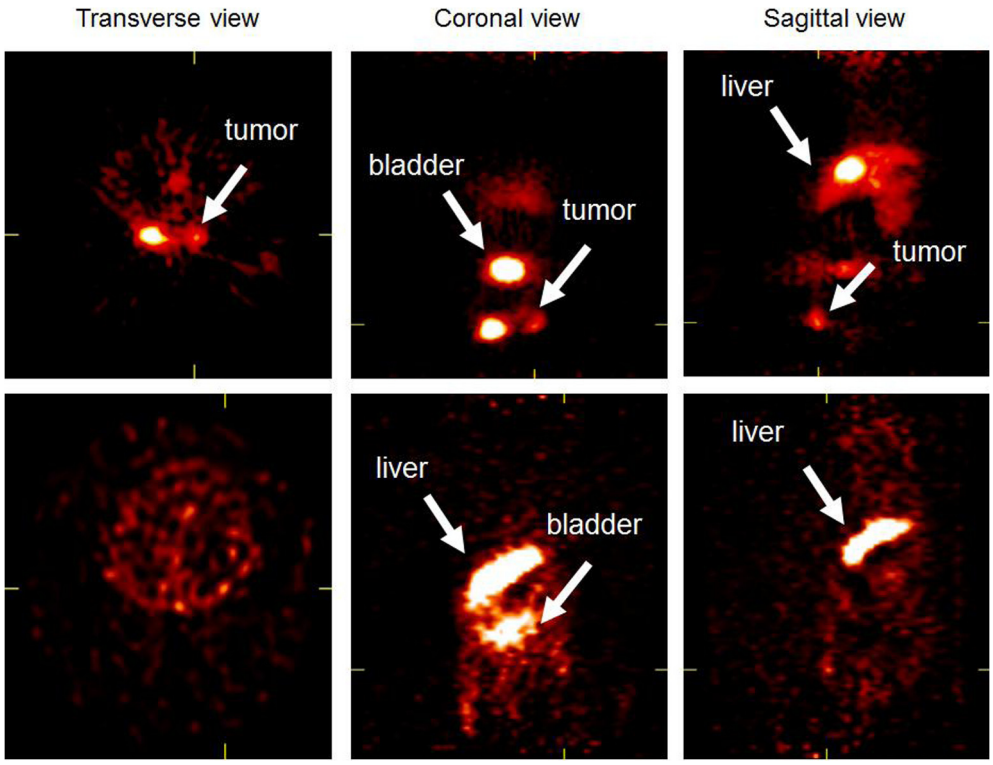

Fig. 3. PET images at 1 h post injection: the upper row shows the tumor uptake in the study group while the bottom row does not show appreciable tumor uptake in the control group. All images are adjusted to the same scale of contrast.

with 100% Solvent A to 20% Solvent A and 80% Solvent B in 12 min, flow rate 1 mL/min) for radiochemistry purity at 99%. The "cold" counterpart of the compound **3** was synthesized and characterized to be used as reference for confirming the compound **3**.

The in vitro stability of the compound **3** was evaluated in mouse serum following a reported procedure.[14] Briefly, to 2 mL mouse serum (Sigma-Aldrich, St. Louis, MO) was added aliquot of 100 μCi tracer and the mixture was incubated at 37 °C. At each time point of 0 h, 0.5 h, 1 h, 1.5 h, 2 h, an aliquot of 250 μL was cooled on ice, mixed with 250 μL ACN/DMSO solution (1:1), vortexed for half minute to precipitate serum protein out, and then centrifuged at 3000 RCF for 3 min. The upper supernatant was analyzed by HPLC. As shown in Fig. 2, there was no appreciable degradation in mouse serum (37 °C) over 2 h. In addition, in PBS (pH 7.4, 37 °C) no appreciable hydrolysis was observed over a period of 12 h.

The newly synthesized probe molecule was initially evaluated for PET imaging mesothelioma in mice. Animal procedures were carried out in compliance with a protocol approved by the University of Virginia, Institutional Animal Care and Use Committee. Four-week-old male *nu/nu* mice were purchased from Charles River Laboratories (Wilmington, MA). For tumor inoculation, 2×10^6 MSTO-211H cell lines in 200 μl PBS were administered by intraperitoneal (IP) injection to the upper right abdomen area of each mice group (n = 4).. Growing tumors were palpated and the diameters were measured by a vernier caliper. The tumor-bearing mice were imaged or used in *ex vivo* biodistribution experiment when tumor size reached about 3–5 mm in diameter.

For PET imaging and biodistribution studies, tumor-bearing mice were given 100 μCi of the compound **3** (1 μg) in 200 μL of saline via intraperitoneal injection for the study group while mice receiving 200 μg unlabeled compound **1** at 1 h before compound **3** for the control group. At time point of 0 h, 0.5 h, 1.5 h, 17.5 h post injection of compound **3**, the mice were scanned with a microPET scanner (Focus F-120, Siemens) under anesthesia with 1.5% to 3% isoflurane in oxygen (v/v) for 30 min. With microPET Manager

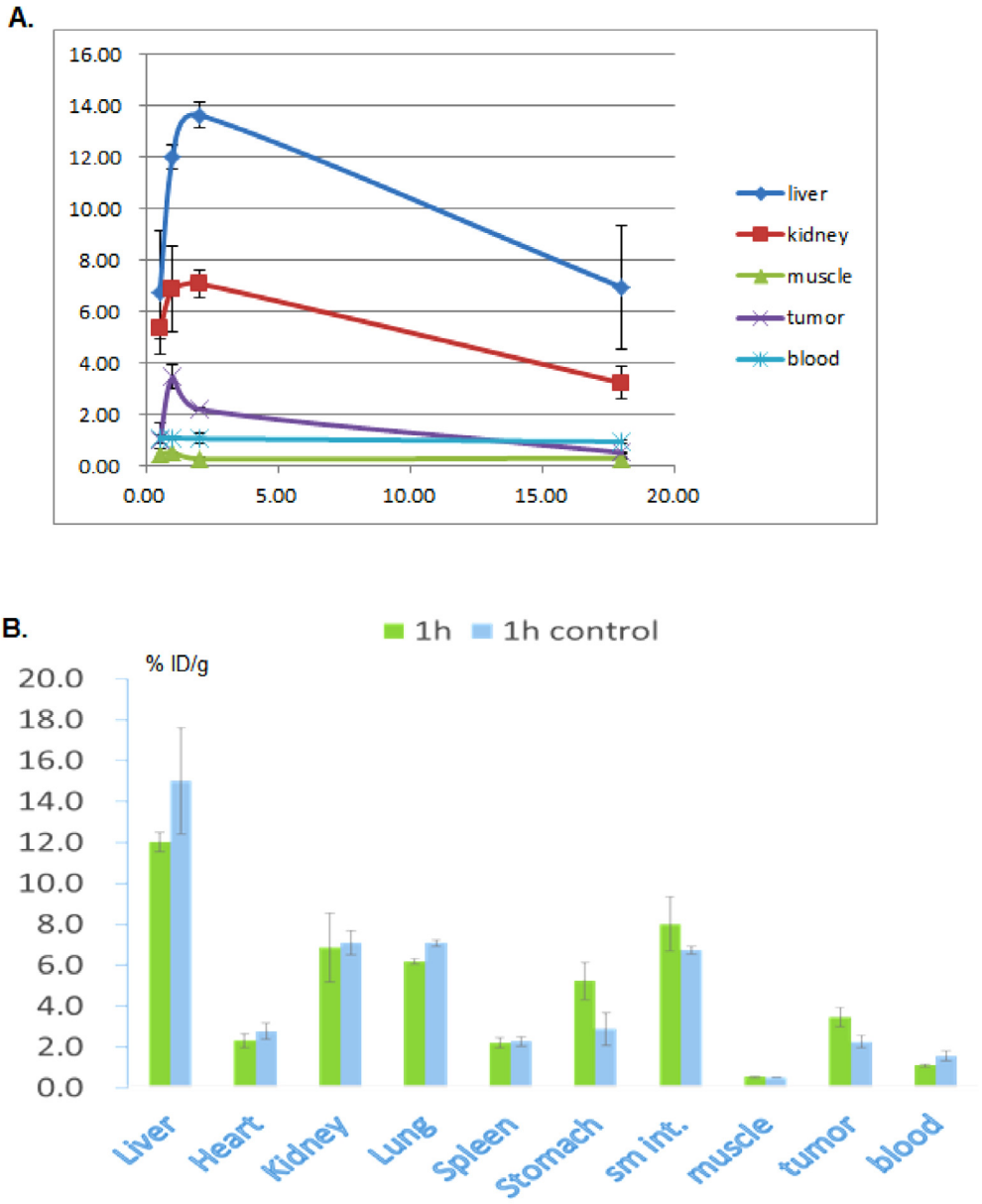

Fig. 4. Biodistribution of the compound **3**: (A) the distribution in liver, kidney, muscle, tumor and blood at time point of 0.5 h, 1 h, 2 h, 18 h post injection of the compound **3**. (B) Biodistribution comparison between the study group and the control group at 1 h post injection of the compound **3**.

(version 2.4.1.1, Siemens), PET data were reconstructed using the OSEM3D/MAP algorithm (zoom factor, 2.164). As shown in Fig. 3 for representative mice (the upper one for the studies mouse and the bottom one for the control), apparent tumor uptake was observed in the studies mouse at the time point of 1 h post injection whereas less appreciable tracer accumulation was seen in the control mouse.

Following the imaging study, each group of mice (n = 4) were sacrificed under anesthesia by cervical dislocation at time point of 0.5 h, 1 h, 2 h, 18 h post injection. The blood was collected by cardiac puncture immediately. Organs including liver, heart, kidney, lung, spleen, stomach, small intestine, muscle and tumors were collected and weighed, and the tissue radioactivities were measured with an automatic gamma counter (2480 Wizzard, PerkinElma). The %ID/g was calculated by comparison with reference samples of measured dose. Data were expressed as mean ± SD. Statistical significance was calculated using a Student's *t*-test and with more than one data sets, ANOVA was used to compare results. A P-value <0.05 was considered significant.

The tumor targeting of Cu-64 labeled PARP probe in vivo was also confirmed by biodistribution studies. As shown in Fig. 4A, the tumor uptake was not apparent at 0.5 h (0.98 ± 0.69% ID/g, compared to muscle 0.47 ± 0.18% ID/g) while it peaked at 1 h (3.45 ± 0.47% ID/g) post injection, which was consistent with PET imaging observation. While the uptake in other normal organs and tissues are comparable between the study group and control group at 1 h post-injection (Fig. 4B), the tumor uptake in the study group is significantly higher than that in control group (3.45 ± 0.47% ID/g vs 2.26 ± 0.30% ID/g).

In conclusion, a modification was made to Olaparib by conjugation with DOTA, followed by radiolabeling with Cu-64. The newly synthesized probe molecule was evaluated in mice with mesothelioma in vivo. The PET imaging showed that tumor could be detected using this tracer, which was confirmed by biodistribution study. These results warrant further development of PARPi-based theranostic probes for PET imaging and radiotherapy for mesothelioma.

Acknowledgements

We would like to thank Dr. James Stone and Dr. Dongfeng Pan for access to lab facilities. We also thank Dr. Bijoy Kundu, Dr. Yi Zhang and Dr. Mahendra Chordia for helpful discussions. Research reported in this publication was partially supported by the National Cancer Institute (CCSG P30 CA44579 and R01CA135358). The content is solely the responsibility of the authors, and does not necessarily represent the official views of the National Institutes of Health.

References

1. D'Amours D, Desnoyers S, D'Silva I, Poirier GG. Poly(ADP-ribosyl)ation reactions in the regulation of nuclear functions. *Biochem J*. 1999;342:249–268.
2. Helleday T, Petermann E, Lundin C, Hodgson B, Sharma RA. DNA repair pathways as targets for cancer therapy. *Nat Rev Cancer*. 2008;8:193–204.
3. Ledermann JA. PARP inhibitors in ovarian cancer. *Ann Oncol*. 2016;27:i40–i44.
4. Ossovskaya V, Koo IC, Kaldjian EP, Alvares C, Sherman BM. Upregulation of poly (ADP-ribose) polymerase-1 (PARP1) in triple-negative breast cancer and other primary human tumor types. *Genes Cancer*. 2010;1:812–821.
5. Rojo F, Garcia-Parra J, Zazo S, et al. Nuclear PARP-1 protein overexpression is associated with poor overall survival in early breast cancer. *Ann Oncol*. 2012;23:1156–1164.
6. Barton VN, Donson AM, Kleinschmidt-DeMasters B, Gore L, Liu AK, Foreman NK. PARP1 expression in pediatric central nervous system tumors. *Pediatr Blood Cancer*. 2009;53:1227–1230.
7. Galia A, Calogero A, Condorelli R, et al. PARP-1 protein expression in glioblastoma multiforme. *Eur J Histochem*. 2012;56:9.
8. Staibano S, Pepe S, Muzio LL, et al. Poly (adenosine diphosphate-ribose) polymerase 1 expression in malignant melanomas from photoexposed areas of the head and neck region. *Hum Pathol*. 2005;36:724–731.
9. Menear KA, Adcock C, Boulter R, et al. 4-[3-(4-Cyclopropanecarbonylpiperazine-1-carbonyl)-4-fluorobenzyl]-2*H*-phthalazin-1-one: a novel bioavailable inhibitor of poly (ADP-ribose) polymerase-1. *J Med Chem*. 2008;51:6581–6591.
10. Keliher EJ, Reiner T, Turetsky A, Hilderbrand SA, Weissleder R. High-yielding, two-step 18F labeling strategy for 18F-PARP1 inhibitors. *ChemMedChem*. 2011;6:424–427.
11. Reiner T, Keliher EJ, Earley S, Marinelli B, Weissleder R. Synthesis and in vivo imaging of a 18F-labeled PARP1 inhibitor using a chemically orthogonal scavenger-assisted high-performance method. *Angew Chem Int Ed*. 2011;50:1922–1925.
12. Reiner T, Lacy J, Keliher EJ, et al. Imaging therapeutic PARP inhibition in vivo through bioorthogonally developed companion imaging agents. *Neoplasia*. 2012;14(3). 169IN1–77IN3.
13. Carlucci G, Carney B, Brand C, et al. Dual-modality optical/PET imaging of PARP1 in glioblastoma. *Mol Imag Biol*. 2015;17:848–855.
14. Irwin CP, Portorreal Y, Brand C, et al. PARPi-FL-a fluorescent PARP1 inhibitor for glioblastoma imaging. *Neoplasia*. 2014;16:432–440.
15. Iyer AK, Su Y, Feng J, et al. The effect of internalizing human single chain antibody fragment on liposome targeting to epithelioid and sarcomatoid mesothelioma. *Biomaterials*. 2011;32:2605–2613.
16. Iyer AK, Lan X, Zhu X, et al. Novel human single chain antibody fragments that are rapidly internalizing effectively target epithelioid and sarcomatoid mesotheliomas. *Cancer Res*. 2011;71:2428–2432.
17. Pinton G, Manente AG, Murer B, Marino E, Mutti L, Moro L. PARP1 inhibition affects pleural mesothelioma cell viability and uncouples AKT/mTOR axis via SIRT1. *J Cell Mol Med*. 2013;17:233–241.
18. Li Z, Conti PS. Radiopharmaceutical chemistry for positron emission tomography. *Adv Drug Deliv Rev*. 2010;62:1031–1051.
19. Connett JM, Anderson CJ, Guo LW, et al. Radioimmunotherapy with a 64Cu-labeled monoclonal antibody: a comparison with 67Cu. *Proc Natl Acad Sci USA*. 1996;93:6814–6818.
20. Anderson RC, Makvandi M, Xu K, et al. Iodinated benzimidazole PARP radiotracer for evaluating PARP1/2 expression in vitro and in vivo. *Nucl Med Biol*. 2016;43:752–758. http://dx.doi.org/10.1016/j.nucmedbio.2016.08.007.